

CrystEngComm

Accepted Manuscript



This is an *Accepted Manuscript*, which has been through the Royal Society of Chemistry peer review process and has been accepted for publication.

Accepted Manuscripts are published online shortly after acceptance, before technical editing, formatting and proof reading. Using this free service, authors can make their results available to the community, in citable form, before we publish the edited article. We will replace this *Accepted Manuscript* with the edited and formatted *Advance Article* as soon as it is available.

You can find more information about *Accepted Manuscripts* in the [Information for Authors](#).

Please note that technical editing may introduce minor changes to the text and/or graphics, which may alter content. The journal's standard [Terms & Conditions](#) and the [Ethical guidelines](#) still apply. In no event shall the Royal Society of Chemistry be held responsible for any errors or omissions in this *Accepted Manuscript* or any consequences arising from the use of any information it contains.

ARTICLE

Bulk crystal growth and characterization of semi-organic nonlinear optical crystal tri-diethylammonium hexachlorobismuthate (TDCB)

Cite this: DOI: 10.1039/x0xx00000x

Received 00th January 2012,
Accepted 00th January 2012

DOI: 10.1039/x0xx00000x

www.rsc.org/

Guangfeng Liu, Jie Liu, Xiaoxin Zheng, Yang Liu,* Dongsheng Yuan, Xixia Zhang, Zeliang Gao, and Xutang Tao*

Bulk semi-organic nonlinear optical (NLO) single-crystals of tri-diethylammonium hexachlorobismuthate (TDCB) with the sizes up to $22 \times 21 \times 15 \text{ mm}^3$ have been grown from concentrated hydrochloric acid by slow-cooling method. TDCB crystallizes in the trigonal system, $R\bar{3}c$ space group, with $a = 14.699(4) \text{ \AA}$, $c = 19.102(5) \text{ \AA}$. Its morphology has been indexed to reveal the major facets of the crystal to be $\{11\bar{2}0\}$ and $\{01\bar{1}2\}$. Transmittance spectra of TDCB show an optical transmission in the entire visible region with the cutoff wavelength at 365 nm. The powder second harmonic generation (SHG) measured by using the Kurtz and Perry technique indicates that TDCB is a phase-matchable NLO materials with a SHG efficiency of 1.8 times as that of KH_2PO_4 (KDP). Its specific heat and the thermal expansion were investigated as a function of temperature, and the relationship between the structure and the thermal properties has been discussed. Furthermore, the laser-induced damage threshold measurements show a threshold up to 2.32 GW cm^{-2} . All the results demonstrate this semi-organic crystal TDCB is promising in NLO applications.

Introduction

Nonlinear optical (NLO) materials have gained great attention because of their importance in laser frequency conversion, optical communication and optical data storage.¹⁻⁴ To meet the needs of these applications, NLO materials with properties such as large optical susceptibilities (χ), higher laser damage resistance, short transparency cutoff wavelengths and stable thermal and mechanical performance are desired. Much effort has been devoted to designing and exploring of novel NLO materials; and numerous inorganic and organic materials with interesting physicochemical property have been studied.⁵⁻⁹ Generally speaking, typical inorganic NLO materials have good mechanical and thermal properties, making the growth and process of large crystals easy; per contra, organic materials possess fast response times, high optical susceptibilities, high laser damage threshold¹⁰⁻¹² and flexible chemical structures, but scarcely any practical usability because of their poor mechanical and thermal stability, and the infeasibility in growing large single crystals.¹³⁻¹⁴ In order to combine both the advantages of inorganic and organic materials, many semi-organic materials with NLO effect have been designed and synthesized, in which the organic and inorganic components crystallize together according to stoichiometric ratios.¹⁵⁻¹⁶

In this context, metal halide anion $(\text{BiCl}_6)^{3-}$ that containing a lone pair of electrons and an asymmetric coordination is believed more prone to induce a noncentrosymmetric space group in crystals. Although several bismuth chloride-based organic inorganic hybrids have been synthesized,¹⁷⁻¹⁹ their bulk single crystals and corresponding properties are scarcely reported. In this work, we took diethylamine as the organic counter cation with hexachlorobismuthate anions to form a hybrid material tri-diethylammonium hexachlorobismuthate (TDCB). Large size TDCB single crystals were successfully grown from concentrated hydrochloric acid by slow-cooling method. Optical and other physical investigations such as transmittance spectra, SHG effect, thermal expansion, and laser-induced damage threshold are reported in detail.

Experimental section

Synthesis and crystal growth

All of the starting materials were analytical-grade reagents from TCI Chemical Company. Commercially available solvents were used as received without further purification. The raw TDCB products were prepared by dissolving $[\text{NH}_2(\text{C}_2\text{H}_5)_2]\text{Cl}$ and $\text{Bi}_2\text{O}_2\text{CO}_3$ with a molar ratio of 6:1 in 36% HCl. The solution was stirred and allowed to evaporate the solvent by vacuum distillation. To improve the purity of the synthesized salt,

recrystallization was performed two times. The identity and purity of the TDCB crystals were verified from the power X-ray diffraction (PXRD) (Fig. S1) and FT-IR spectra (Fig. S2). In order to optimize the single crystal growth conditions, the solubilities of TDCB in 36% HCl in the temperature range from 30 to 50 °C were determined by the gravimetric method. The result is shown in Fig. 1, which indicates a relative small solubility of TDCB with a positive solubility temperature gradient in saturated HCl solution. Before the bulk crystal growth, small crystals with good quality and well-defined shapes obtained by spontaneous crystallization were selected as the seeds. To make sure the saturation of TDCB in concentrated HCl solution, it was maintained at 50 °C for 3 days; then the seed crystal mounted on a plastic holder was dipped to the solution. The temperature was reduced at a rate of 0.1 °C/day within the first 5 days, and subsequently 0.5 °C/day as the growth progressed. In a period of about 40 days, colorless transparent single crystals with the size up to $22 \times 21 \times 15 \text{ mm}^3$ were obtained. Fig. 2 presents an as-grown TDCB crystal and a polished sample. Its morphology is deduced from BFDH theory according to the structure data.²⁰⁻²¹ The ideal crystal morphology of TDCB is a dodecahedron with six top/bottom and six side faces. In the as-grown crystals, the developed facets are $\{11\bar{2}0\}$ and $\{01\bar{1}2\}$, being consistent with the BFDH results.

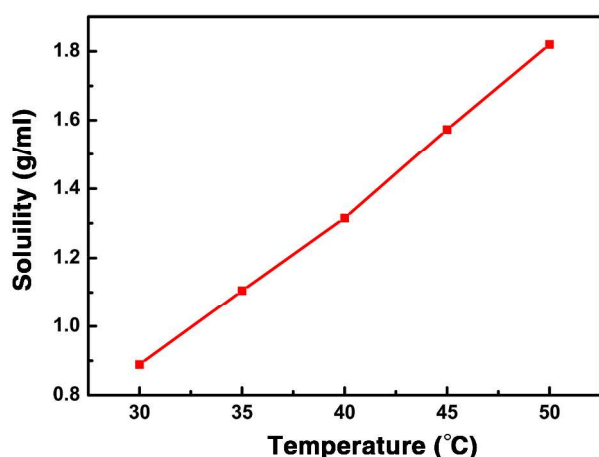


Fig.1 Solubility curve of TDCB in concentrated hydrochloric acid (36%).

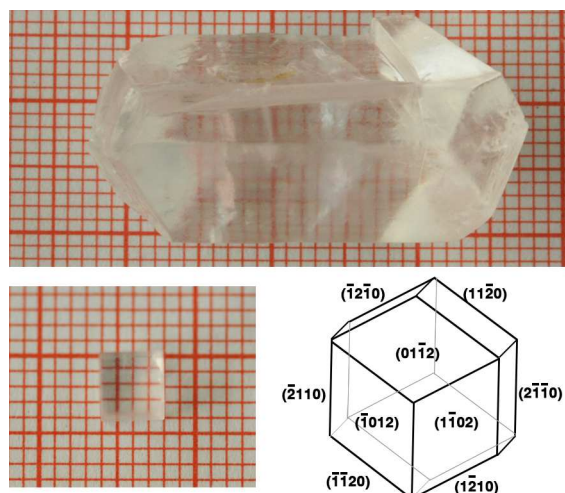


Fig.2 Photos of an as-grown single crystal and a cut sample from TDCB crystal, and the predicted crystal morphology based on the BFDH method.

Characterization techniques

Powder X-ray Diffraction. The powder X-ray diffraction was performed on a Bruker D8 ADVANCE X-ray diffractometer equipped with a diffracted beam monochromator set for Cu K α radiation ($\lambda = 1.54056 \text{ \AA}$) in the 2θ range 10–50°, with a step size of 0.02° and a step time of 0.2 s at room temperature.

Single-crystal X-ray Diffraction. A block-shaped single-crystal of TDCB ($0.42 \text{ mm} \times 0.41 \text{ mm} \times 0.35 \text{ mm}$) was selected for single-crystal X-ray data collection with a Bruker SMART APEXII CCD area detector on a D8 goniometer at 100 K. Data were collected using graphite-monochromated and 0.5 mm-Mono Cap-collimated Mo-K α radiation ($\lambda = 0.71073 \text{ \AA}$) with the ω scan method. Data were processed with the INTEGRATE program of the APEX2 software for reduction and cell refinement. Multi-scan absorption corrections were applied by using the SCALE program for area detector. The structure was solved by the direct method and refined by the full-matrix least-squares method on F^2 (SHELX-97).²² All non-H atoms were refined anisotropically. Hydrogen atoms were placed in idealized positions and included as riding with $U_{\text{iso}}(\text{H}) = 1.2 U_{\text{eq}}(\text{C})$.

Optical Measurements. The attenuated total reflectance Fourier transform infrared spectra (ATR-FTIR) of powders of TDCB was recorded on a Thermo-Nicolet NEXUS 670 spectrometer in the range 700–4,000 cm^{-1} at room temperature. The optical transmission spectra of a TDCB single crystal with the thickness of 4.0 mm was recorded using a Hitachi U-3500 UV-Vis-NIR spectrometer from the range 200–1500 nm at room temperature. SHG measurement was performed on a modified Kurtz-NLO system using a Q-switched Nd:YAG laser of wavelength 1064 nm with a pulsed beam (10 ns, 3 mJ, 10 Hz).²³ Polycrystalline samples of TDCB were ground and sieved into distinct particle size in the range of 25–125 μm . The sieved KDP powders were used as a reference.

Thermal Measurements. Specific heat was measured under a nitrogen atmosphere in the range from 293 to 380 K on a Perkin-Elmer Diamond DSC analyser. Differential scanning calorimetry (DSC) and thermogravimetric analysis (TGA) for TDCB were carried out on a TGA/DSC/1600HT analyzer (METTLER TOLEDO Instruments). The sample was placed in Al_2O_3 crucible, and heated at a rate of 10 K min^{-1} from room temperature to 650 K under flowing nitrogen gas. Thermal expansion of the TDCB crystal was measured with the temperature up to 352 K on a Perkin-Elmer thermal dilatometer (Diamond TMA), by using two cut and polished cubic samples with size of $4 \times 4 \times 4 \text{ mm}^3$. The faces of (0001) and (1120) were determined by X-ray diffraction. Laser-induced damage threshold measurement was carried out on the (0001) plane of the crystal using an Nd:YAG laser (1064 nm) with the frequency 1 Hz and the pulse width 8 ns.

Hardness. The mechanical resistance of TDCB crystal was estimated with an HXD-1000C micro-hardness tester on (0001) and (1120) faced polished wafers with dimensions of $4 \times 4 \times 2 \text{ mm}^3$. The indentation load was 25 g and the selected time was 2 s. Three test points were performed per sample to obtain the

average value. The micro-hardness (H_v) and Mohs hardness (H_M) values were calculated using the relation: $H_v = 1.8544 \times (p/d^2)$ kg mm⁻²; $H_M = 0.675 \times (H_v)^{1/3}$ where p is the load pressure and d is the diagonal length of the indentations marked on wafer surface.

Results and discussion

Crystal structure analysis

The crystal structure of TDCB is shown in Fig. 3. The crystal belongs to trigonal system with space group of $R\bar{3}c$ and the unit cell parameters of $a = 14.699(4)$ Å, $c = 19.102(5)$ Å, and $V = 3574.25$ Å³ (Table S1), which agrees well with the reported values.²⁴ As shown in Fig. 3a, each Bi atom is connected by six Cl atoms of the ligands. There are two different Bi-Cl bonds (Cl_1 -Bi = 2.598 Å and Cl_2 -Bi = 2.867 Å) in a bismuth chloride anion, which distort the $BiCl_6^{3-}$ octahedron. Fig. 3b shows the interactions between $BiCl_6^{3-}$ anions and diethylammonium cations. Specifically, Cl_1 atoms connect to diethylammonium cations via weaker N-H...Cl ($d/\text{Å}$, $\theta/^\circ$: 2.91, 119.4) hydrogen bonds; while Cl_2 atoms connect to diethylammonium cations via relatively stronger N-H...Cl ($d/\text{Å}$, $\theta/^\circ$: 2.41, 154.5) and N...Cl (3.256 Å) hydrogen bonds. The distortion of the $BiCl_6^{3-}$ octahedron is in favor of the SHG response of TDCB. Fig. 3c and 3d illustrate the packing representation of the TDCB crystal viewed along the a -axis and c -axis, respectively. It can be found that the $BiCl_6^{3-}$ anions stack in the (1000) plane more closely than in the (0001) plane, which would result in different mechanical and thermal properties of the crystals in different directions.

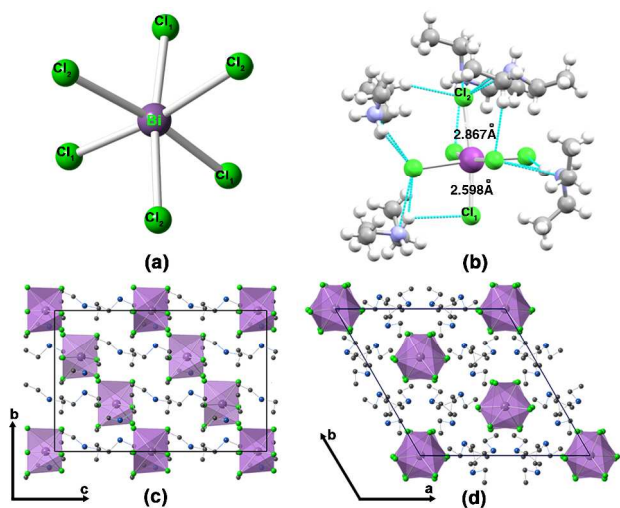


Fig.3 Crystal structure of TDCB: (a) $BiCl_6$ octahedron; (b) interactions between $BiCl_6^{3-}$ anions and diethylammonium cations; (c) view of the crystal structure along a axis; (d) view of the crystal structure along c axis. $BiCl_6$ octahedron is shown in lavender. Colour scheme: Bi (III), purple; Cl, green; C, grey; N, blue; H, white.

Transmission spectrum

The transmission spectrum of the TDCB crystal along c -axis is shown in Fig. 4. It displays a UV transparency cutoff wavelength of 365nm, which is in agreement with the crystal's

colorlessness. The transparency range of the crystal is from 380 nm to 1100 nm, which is an advantage for the NLO applications,²⁵ e.g., no apparent absorbance for the SHG and self-frequency doubling (SFD) of 1064 nm laser.

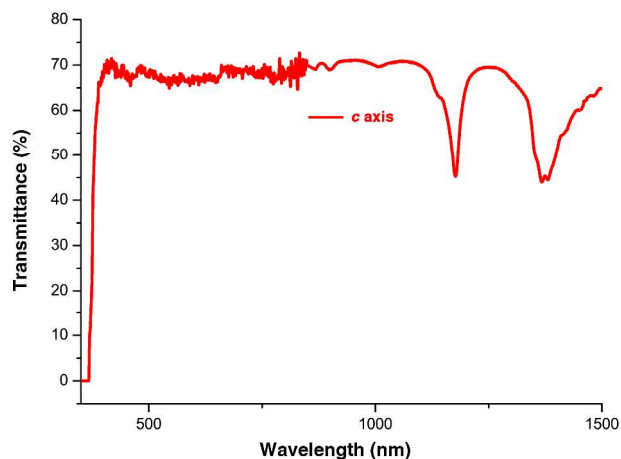


Fig.4 Transmission spectrum of TDCB crystal along the c axis.

Kurtz-Perry powder SHG measurements

Because of the non-centrosymmetry of TDCB crystal, it is expected to possess NLO properties. The NLO ability of the TDCB crystal powder is estimated by Kurtz-Perry powder SHG measurements. As shown in Fig. 4, the second-harmonic intensity increases with particle size and saturation at a maximum value, indicating TDCB is phase-matchable. Comparison of the second-harmonic produced by TDCB and KDP in the same particle range reveals that the SHG efficiency of TDCB is 1.8 times as large as that of KDP. This value is comparable with that of another bis thiourea bismuth chloride (BTBC),²⁶ which should be attributed to the distortion of the $BiCl_6^{3-}$ octahedron.

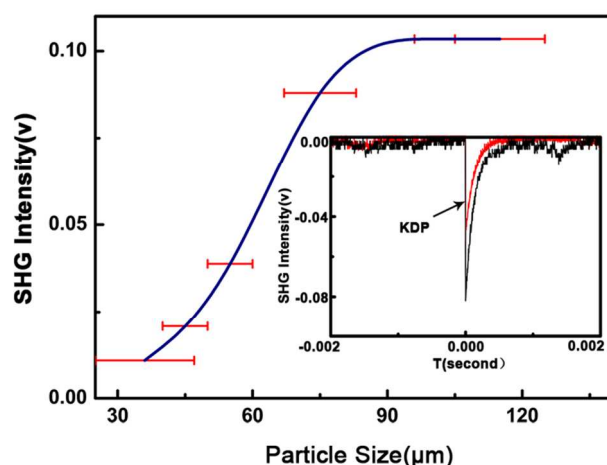


Fig.5 Second-harmonic intensity of TDCB powders as a function of particle size. The inset is the comparative SHG oscilloscope traces of the powder samples with the same particle sizes of, KDP (red) and TDCB (black).

Specific heat and thermogravimetric analysis

For NLO applications, the specific heat of a crystal is one of the important factors which influences greatly the damage threshold. A material with higher specific heat generally has more resistance to laser damage. Fig. 6 shows the specific heat vs temperature curve of a TDCB crystal. It can be seen that the specific heat of TDCB crystal increases almost linearly from 1.05 to 1.42 J g⁻¹ K⁻¹ in the measured temperature range from 295 to 380 K, similar to those of other organic and inorganic crystals.²⁷⁻²⁸ TG curve for TDBC (Fig. S3) shows no obvious weight loss before 500K; and the DSC curve shows three endothermic reactions before weight loss at 426 K, 442 K and 448 K, which may be assigned to some phase transitions and the melting of the material.

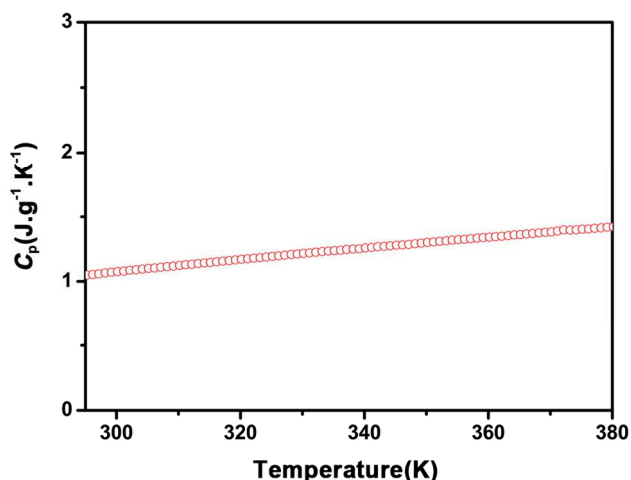


Fig.6 Dependence of the specific heat of TDCB crystal with temperature.

Thermal expansion

The thermal expansion of a crystal is another basic property that influences crystal growth and laser applications.²⁹ For the trigonal TDCB crystal, the thermal expansion coefficient tensor with respect to the axes in the conventional orientation is as below.³⁰

$$\begin{pmatrix} \alpha_{11} & 0 & 0 \\ 0 & \alpha_{11} & 0 \\ 0 & 0 & \alpha_{33} \end{pmatrix}$$

There are two independent principal thermal components, α_{11} and α_{33} . In order to determine α_{ij} , a sample along a and c vector directions was cut from the as-grown crystal (inset of Fig. 7). Fig. 7 shows the relative thermal expansion curves along the two different orientations. It can be seen that the relative thermal expansion is almost linear over the entire measured temperature. The average expansion coefficients along the two different orientations can be calculated according to the following formula:

$$\alpha_i(T_0 \rightarrow T) = \frac{\Delta L}{L_0} \frac{1}{\Delta T}$$

where $\alpha_i(T_0 \rightarrow T)$ is the average linear thermal expansion along the measured orientation over the temperature range from T_0 to T . The resulted average linear thermal expansion coefficients of the TDCB crystal along a and c axes over the temperature range 300 to 352 K are $\alpha_{11} = 2.308 \times 10^{-5} \text{ K}^{-1}$ and $\alpha_{33} = 1.653 \times 10^{-4} \text{ K}^{-1}$, respectively.

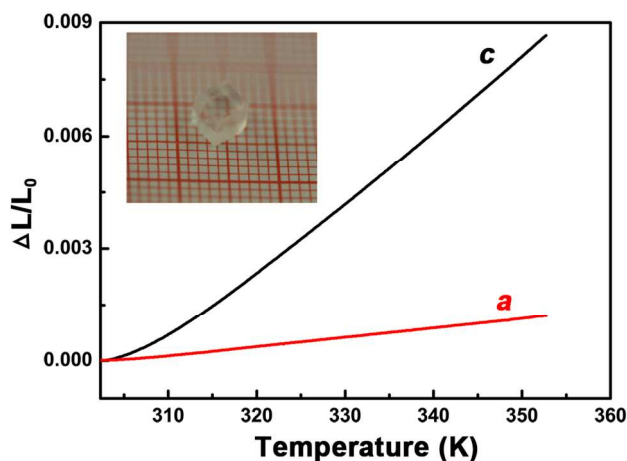


Fig.7 Relative thermal expansion curves along a and c orientations.

The relationship between crystallographic orientation and the thermal expansion orientation is demonstrated in Fig 8. The thermal expansion can be interpreted according to its crystal structure. As shown in Fig. 3c and 3d, the stack of the asymmetric BiCl_6^{3-} octahedron is related by the 3-fold screw axis, leading to a looser stacking of anions along c -axis than that along a -axis. For hybrid materials, the mechanical and thermal properties mainly depend on the inorganic components; therefore, the thermal expansion coefficient α_{11} is smaller than that of α_{33} .

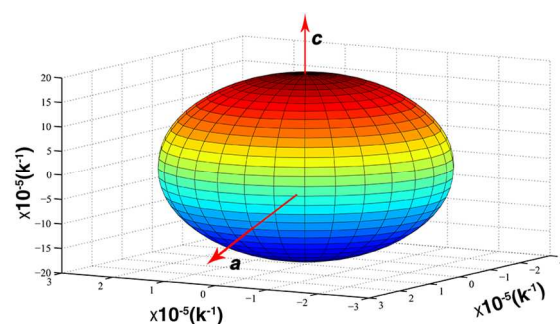


Fig.8 Thermal expansion ellipsoid of TDCB crystal.

Laser damage threshold

The laser-induced damage threshold measurement for TDCB single crystal was carried out on a crystal plate with the thickness of 4 mm using a high-powder laser beam with an energy of 210 mJ and the diameter of 1.20 mm (1 Hz and the pulse width 8 ns). The laser damage threshold of the crystal can be evaluated by the following equation:

$$I = \frac{E}{tA} = \frac{E}{t \frac{\pi d^2}{4}} = \frac{4E}{t\pi d^2}$$

Where I is the energy required to cause damage, E is the single pulse energy, t is the pulse width, A and d are the area and diameter of the circular spot, respectively. The laser damage energy density was found to be 2.32 GW cm⁻². Although direct comparison of the laser-induced damage thresholds in different reports is unreasonable due to the differences in the testing conditions, such as wavelength and pulse widths,³¹ according to the fact that longer pulses prevent any thermal relaxation and reduce the damage resistance, the measured value for TDCB can be roughly compared with a few known NLO crystals [BBO (2.6 GW cm⁻² at 1064 nm and 10 ns), LHPP (3.02 GW cm⁻² at 1064 nm and 8.3 ns), MHBA (2 GW cm⁻² at 1064 nm and 10 ns), LATF (3.5 GW cm⁻² at 1064 nm and 10 ns), KTP (1.5-2.2 GW cm⁻² at 1064 nm and 11 ns)].³²⁻³⁴ An optical photograph of the damaged TDCB crystal by laser beam is shown in Fig. S4. It shows some blobs and cracks surrounding the core of the damage, indicating the damage is mainly triggered by thermal effects such as anisotropic thermal expansion or melting of the material.

Hardness

The H_v hardness values determined by micro-hardness tester on (0001) and (1120) faces of TDCB crystal were found to be 13.19 and 13.88 kg mm⁻², corresponding to the Mohs hardness value as 1.59 and 1.62, respectively, a little higher than those of some organic NLO crystals such as urea (H_v 6.5-11 kg mm⁻²) and N-methyl urea (H_v 12 kg mm⁻²).³⁵

Conclusions

Bulk semi-organic single-crystals of TDCB containing bismuth chloride anion and diethylammonium cation were grown using the controlled temperature cooling method in concentrated hydrochloric acid. The hybrid crystal has a low cutoff wavelength at 365nm and the second-order NLO efficiency is 1.8 times as large as that of the standard KDP. The thermal properties of TDCB crystal were studied by measuring the thermal expansion, specific heat and thermogravimetric analysis. The laser-induced damage threshold value is relatively high as 2.32 GW cm⁻². These results indicate that the TDCB crystal may be a promising NLO material.

Acknowledgements

The authors greatly thank Qingming Lu and Professor Wentao Yu, for their kind help in the crystal processing and structure refinement, respectively. We thank the National Natural Science Foundation of China (grant no. 51321091, 51227002, 51272129) and the Program of Introducing Talents of Disciplines to Universities in China (111 program no. b06015).

References

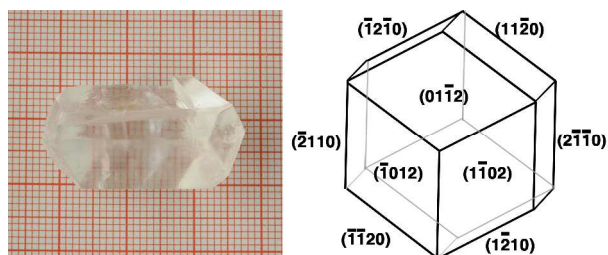
- V. G. Dmitriev, G. G. Gurzadyan and D. N. Nicogosyan, *Handbook of Nonlinear Optical Crystals*, Springer-verlag, New York, 1999.
- E. Ishow, C. Bellaïche, L. Bouteiller, K. Nakatani and J. A. Delaire, *J. Am. Chem. Soc.*, 2003, 125, 15744.
- M. S. Wong, C. Bosshard, F. Pan and P. Gunder, *Adv. Mater.*, 1996, 8, 677.
- L. R. Dalton, P. A. Sullivan, B. C. Olbricht, D. H. Bale, J. Takayesu, S. Hammond, H. Rommel, and B. H. Robinson, *Tutorials in Complex Photonic Media*; SPIE: Bellingham, WA, 2007.
- X. Liu, X. Wang, X. Yin, S. Liu, W. He, L. Zhu, G. Zhang and D. Xu, *CrystEngComm*, 2014, 16, 930.
- W. Zhang, X. Tao, C. Zhang, H. Zhang and M. Jiang, *Crystal Growth & Design*, 2009, 9, 2633.
- L. Kang, Z. Lin, J. Qin and C. Chen, *Sci. Rep.*, 2013, 3, 1366.
- H. J. Zhao, Y. F. Zhang and L. Chen, *J. Am. Chem. Soc.*, 2012, 134, 1993–1995.
- D. Yuan, Z. Jia, J. Wang, Z. Gao, J. Zhang, X. Fu, J. Shu, Y. Yin, Q. Hu and X. Tao, *CrystEngComm*, 2014, 16, 4008.
- W. Zhang and R.-G. Xiong, *Chem. Rev.*, 2011, 112, 1163.
- H. Zhao, Z.-R. Qu, H.-Y. Ye and R.-G. Xiong, *Chem. Soc. Rev.*, 2008, 37, 84.
- Z. Sun, S. Li, S. Zhang, F. Deng, M. Hong and J. Luo, *Adv. Optical. Mat.*, 2014, DOI: 10.1002/adom.201400301.
- H. O. Marcy, M. J. Rosker, L. F. Warren, P. H. Cunningham, C. A. Thomas, L. A. Deloach, S. P. Velsko, C. A. Ebberts, J. H. Liao, and M. G. Kanatzidis, *Opt. Lett.*, 1995, 20, 252.
- R. Mohan Kumar, D. Rajan Babu, and G. Ravi, R. Jayavel, *J. Cryst. Growth.*, 2003, 250, 113.
- S. R. Marder, J. W. Perry and W. P. Schaefer, *Science*, 1989, 245, 626.
- V. Venkataraman, G. Dhanraj, V. K. Wadhawan, J. N. Sherwood, Bhat, H. L. *J. Cryst. Growth.*, 1995, 154, 92.
- G. Xu, Y. Li, W.-W. Zhou, G.-J. Wang, X.-F. Long, L.-Z. Cai, M.-S. Wang, G.-C. Guo, J.-S. Huang, G. Bator and R. Jakubas. *J. Mater. Chem.*, 2009, 19, 2179.
- R. Jakubas, A. Piecha, A. Pietraszko and G. Bator, *Phys. Rev. B.*, 2005, 72, 104107.
- A. Samet, H. Boughzala, H. Khemakhem and Y. Abid, *J. Mol. Struct.* 2010, 984, 23.
- A. Bravais, *Etudes Crystallographiques; Academie des Sciences: Paris*, 1913.
- G. D. H. Donnay, D. Harker, *Am Mineral*, 1937, 22, 446.
- G. M. Sheldrick, *Acta. Crystallogr.* 2008, A64, 112.
- S. K. Kurtz and T. Perry, *J. Appl. Phys.*, 1968, 39 3798.
- S. Jarraya, A. B. Salah and A. Daoud, *Acta Crystallogr.*, 1993, C49, 1594.
- C. Ji, T. Chen, Z. Sun, Y. Ge, W. Lin, J. Luo, Q. Shi and M. Hong, *CrystEngComm*, 2013, 15, 2157.
- R. Sankar, C. M. Raghavan and R. Jayavel, *Crystal Growth & Design*, 2007, 7, 501.
- T. Chen, Z. Sun, C. Song, Y. Ge, J. Luo, W. Lin and M. Hong, *Crystal Growth & Design*, 2012, 12, 2673
- S. Vanishri, J. N. Babureddy, H. L. Bhat and S. Ghosh, *Appl. Phys. B.*, 2007, 88, 457.

- 29 A. K. Burnham, M. Runkel, M. D. Feit, A. M. Rubenchik, R. L. Floyd, T. A. Land, W. J. Siekhaus and R. A. Hawley-Fedder, *Appl. Opt.*, 2003,42, 5483.
- 30 T. Hahn, U. Shmueli, A. A. J. C. Wilson and E. Prince, *International tables for crystallography*, D. Reidel Publishing Company, 2005
- 31 S. Manivannan, S. Dhanuskodi, S. K. Tiwari and J. Philip, *Appl. Phys. B: Lasers Opt.*, 2008, 90, 489.
- 32 D. N. Nikogosyan, *Nonlinear Optical Crystals: A Complete Survey*, Springer, New York, 2005.
- 33 A. Zhang, D. Yuan, X. Tao, D. Xu, Z. Shao, M. Jiang and M. Liu, *Opt. Commun.*, 1993, 99, 247.
- 34 D. Xu, X. Q. Wang, W. T. Yu, S. X. Xu and G. H. Zhang, *J. Cryst. Growth.*, 2003, 253, 481.
- 35 E. E. A. Shepherd, J. N. Sherwood, G. S. Simpson, *J. Cryst. Growth.*, 1996, 167, 709.

State Key Laboratory of Crystal Materials, Shandong University, No. 27 Shanda Nanlu, Jinan, 250100, P. R. China. E-mail: liuyangicm@sdu.edu.cn, txt@sdu.edu.cn; Fax: +86 531 88364518, +86 531 88574135; Tel: +86 531 88369099, +86 531 88364963

† Electronic supplementary information (ESI) available: PXRD pattern, FT-IR spectra, CIF file, TG curves and an optical micrograph for laser damage threshold. CCDC 1031018. For ESI and crystallographic data in CIF or other electronic format see DOI: 10.1039/b000000x/.

TOC:



A promising NLO crystal of tri-diethylammonium hexachlorobismuthate (TDCB) has been grown in large scale; thermal and optical properties were measured.